Title	Piecewise-polynomial associated transform macromodeling algorithm for fast nonlinear circuit simulation
Author(s)	Zhang, Y; Fong, N; Wong, N
Citation	The 18th Asia and South Pacific Design Automation Conference (ASP-DAC 2013), Yokohama, Japan, 22-25 January 2013. In Conference Proceedings, 2013, p. 515-520
Issued Date	2013
URL	http://hdl.handle.net/10722/189852
Rights	Asia and South Pacific Design Automation Conference Proceedings. Copyright © IEEE.

Piecewise-Polynomial Associated Transform Macromodeling Algorithm for Fast Nonlinear Circuit Simulation

Yang Zhang, Neric Fong and Ngai Wong
Department of Electrical and Electronic Engineering
The University of Hong Kong
{yzhang,nfong,nwong}@eee.hku.hk

Abstract — We present a piecewise-polynomial based associated transform algorithm (PWPAT) for macromodeling nonlinear circuits in system-level circuit design. The generated reduced model can provide both global and local accuracies with the most compact dimension. Numerical examples compare it with existing algorithms and verify its superior accuracy in higher order harmonics simulation over traditional Trajectory Piecewise-Linear (TPWL) approach.

I. Introduction

The latest electronic systems are integrating more and more complex functions into a small package. To fulfill the strict design requirements, comprehensive system-level circuit simulation is necessary during the design phase. This is usually performed in a hierarchical style: each functional block is firstly abstracted as a macromodel, then all the macromodels are interconnected to carry out the full-system simulation. Whatever circuit simulator is employed, a circuit macromodel can generally be expressed as a nonlinear ordinary difference equation (ODE),

$$\begin{aligned} E\frac{dx}{dt} &= f\left(x\left(t\right)\right) + Bu\left(t\right) \\ y\left(t\right) &= Cx\left(t\right) \end{aligned} \tag{1}$$

where $E \in \mathbb{R}^{n\times n}$, $B \in \mathbb{R}^{n\times m}$, $C \in \mathbb{R}^{p\times n}$, $x\left(t\right) \in \mathbb{R}^{n}$ is the state variable, $u\left(t\right) \in \mathbb{R}^{m}$ is the input and $y\left(t\right) \in \mathbb{R}^{p}$ is the output. Since the order n is determined by the number of nodes in the circuit and the simulation runtime is generally proportional to n^3, if a circuit consists of a large number of passive and active devices (e.g., a post-layout simulation with back-annotated parasitics), it will consume vast computation resources and take a long time to simulate. Under these circumstances, a model order reduction (MOR) procedure is preferred to downsize the state dimension of the circuit model, i.e., to generate another ODE,

$$\begin{aligned} \hat{E}\frac{dz}{dt} &= \hat{f}\left(z\left(t\right)\right) + \hat{B}u\left(t\right) \\ y\left(t\right) &= \hat{C}z\left(t\right) \end{aligned} \tag{2}$$

where the reduced matrices $\hat{E} \in \mathbb{R}^{q\times q}$, $\hat{B} \in \mathbb{R}^{q\times m}$, $\hat{C} \in \mathbb{R}^{p\times q}$ and $z\left(t\right) \in \mathbb{R}^{q}$, with $q \ll n$. Moreover, the electrical relationships between input nodes and output nodes should be preserved as much as possible.

Linear and weakly nonlinear MOR techniques have been studied extensively in recent years [1–6]. However, most practical circuits show strongly nonlinear relations. To accurately capture these systems, trajectory piecewise methods are proposed to divide the whole solution state space into multiple segments. In each of these segments, the system is approximated by a linear or weakly nonlinear ODE. And then MOR is performed in each of these ODEs to generate their corresponding reduced ODEs. Finally, the combination of these segments in a proper way constitutes the solution of the original problem. This is the intuitive understanding of the Trajectory Piecewise-Linear (TPWL) [7] or Piecewise-Polynomial (PWP) [8] approaches to achieve strongly nonlinear macromodeling.

In these two piecewise methods, TPWL employs linear MOR techniques to model each segment, and PWP needs more complex weakly nonlinear MOR (NMOR) techniques to generate the macromodels of each segment. Most popular NMOR techniques employ moment matching MOR, i.e., finding a projection matrix which projects the original bigger coefficient matrices E, $f\left(\cdot\right)$, B and C into smaller coefficient matrices $\hat{E}$, $\hat{f}\left(\cdot\right)$, $\hat{B}$ and $\hat{C}$. Representative algorithms are NORM [6] and the algorithms in [9] and [10]. In [11], a novel NMOR algorithm was proposed based on associated transform of multivariate Laplace-domain high-order Volterra transfer functions, resulting in generally much more compact reduced models. In this paper, we successfully adapt associated transform algorithm into PWP method, named piecewise-polynomial associated transform (PWPAT), to find more efficient reduced macromodels. Compared to TPWL, the model reduced by the proposed algorithm demonstrates much higher accuracy in higher order harmonics, which is critical for analog or radio-frequency (RF) circuit design. In the mean time, dimension of the reduced model is the most compact via PWPAT.

The paper is organized as following. In Section II, backgrounds of TPWL, PWP, associated transform etc., are reviewed. And then the detailed PWPAT algorithm is introduced in Section III. Section IV presents numerical examples to contrast with existing algorithms. Finally, Section V draws the conclusion.

II. Background

A. TPWL and PWP algorithms

TPWL algorithm, such as [7, 8, 12, 13], is widely used in strongly NMOR in which linear MOR is performed in each piecewise segment. The algorithm is outlined as follows:

978-1-4673-3030-5/13/$31.00 ©2013 IEEE

1. Given a nonlinear system of (1), linearize it at various expansion states points $x_i, i = 1, 2, \cdots, k$,

$$\begin{aligned} E\dot{x} &= f(x_i) + A_i(x - x_i) + Bu \\ y &= Cx. \end{aligned} \tag{3}$$

2. Generate a projection basis V_i through Arnoldi process for each segment and calculate a common orthonormal basis V via $[V_1 V_2 \cdots V_k]$, where $V \in \mathbb{R}^{n\times q}$.

3. Perform linear MOR on each segment using V, which reduces (3) into

$$\begin{aligned} \hat{E}\dot{z} &= \hat{f}(x_i) + \hat{A}_i(z - z_i) + \hat{B}u \\ y &= \hat{C}z \end{aligned} \tag{4}$$

where the reduced matrices $\hat{E} \in \mathbb{R}^{q\times q}$, $\hat{A}_i \in \mathbb{R}^{q\times q}$, $\hat{B} \in \mathbb{R}^{q\times m}$ and $\hat{C} \in \mathbb{R}^{p\times q}$.

4. The final reduced model is the weighted combination of all the reduced models

$$\begin{aligned} \hat{E}\dot{z} &= \sum_{i=1}^{s} \omega_i(z)\left(\hat{f}(x_i) + \hat{A}_i(z - z_i) + \hat{B}u\right) \\ y &= \hat{C}z \end{aligned} \tag{5}$$

where $\omega_i(z)$ is the weight function, which can be obtained with the approach in [7].

However, since TPWL algorithm divides the whole state space into small segments and uses first-order approximation in each segment, this algorithm can only provide global accuracy. In some practical simulation with interests in higher order harmonics, the macromodels generated by TPWL algorithm are insufficient and produce large errors. Therefore a method which provides both global and local accuracies is desired. In [8], a general form of TPWL, the PWP, is proposed. As shown in Fig.1, its improvement compared to traditional TPWL is that in each segment of the state space, higher order approximation is employed to replace the first-order approximation. Hence, both global and local accuracies are preserved, and the higher order harmonics can be accurately captured in the simulations by the generated macromodels.

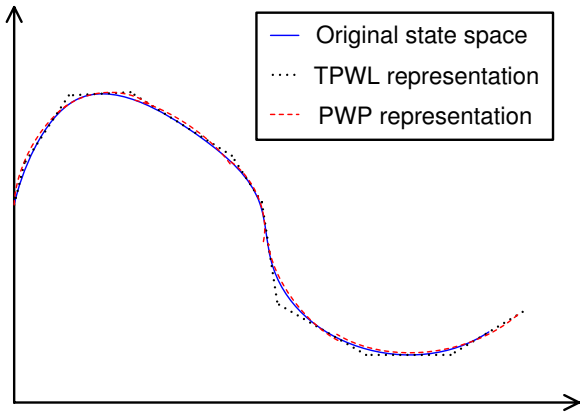

Fig. 1. TPWL and PWP representations of a nonlinear system in a two-dimensional state space.

B. NMOR by associated transform

In each segment of the state space, the input-output relationships can be described by an ODE. For example, consider one segment with a quadratic relation

$$\begin{aligned} E\dot{x} &= G_1 x + G_2 x \otimes x + Bu \\ y &= Cx, \end{aligned} \tag{6}$$

where $G_i = \frac{1}{i!}\frac{\partial^i f}{\partial x^i}\Big|_{x=x_0} \in R^{n\times n^i}$ and $\otimes$ denotes the Kronecker product. By Volterra theory, the 1st- to 3rd-order transfer functions of (6) can be obtained,

$$H_1(s) = (sE - G_1)^{-1} b \tag{7a}$$

$$\begin{aligned} H_2(s_1, s_2) = \frac{1}{2}\left((s_1 + s_2)E - G_1\right)^{-1} \{G_2[H_1(s_1) \\ \otimes H_1(s_2) + H_1(s_2) \otimes H_1(s_1)]\} \end{aligned} \tag{7b}$$

$$\begin{aligned} H_3(s_1, s_2, s_3) = \frac{1}{3}\left((s_1 + s_2 + s_3)E - G_1\right)^{-1} \cdot \\ \{G_2[H_1(s_1) \otimes H_2(s_2, s_3) + H_2(s_2, s_3) \otimes H_1(s_1) \\ + H_1(s_2) \otimes H_2(s_1, s_3) + H_2(s_1, s_3) \otimes H_1(s_2) \\ + H_1(s_3) \otimes H_2(s_1, s_2) + H_2(s_1, s_2) \otimes H_1(s_3)]\}. \end{aligned} \tag{7c}$$

Traditionally, with the existing weakly NMOR algorithms such as [6, 9, 10], a projection matrix $V \in R^{n\times q}$ in which $q \ll n$ can be generated by moments matching of all the Laplace coefficients $1, s_1, s_2, s_3, s_1^2, s_1 s_2, s_1 s_3, s_2^2, s_2 s_3, s_3^2 \cdots$. And the reduced system will be constructed via this projection matrix. However, these Laplace coefficients $s_1, s_2, s_3 \cdots$ are corresponding to multi-time coefficients $t_1, t_2, t_3 \cdots$ by multidimensional inverse Laplace transform. The time-domain results are obtained from the unification of all these multi-time coefficients, i.e., $h_n(t) = h_n(t_1, \cdots, t_n)|_{t_1=t_2=\cdots=t_n=t}$. Therefore, there are some redundancies if moments matching are performed with all the Laplace coefficients taken into account.

The theory of association of variables $\mathscr{A}_n$ was firstly developed to unify these Laplace coefficients in the frequency domain [14], i.e., by converting the Laplace coefficients $s_1, s_2, s_3 \cdots$ into a single s ahead of the moment matching, the generated reduced system has the most compact dimension. This is especially desirable in piecewise based methods since the assembled system consists of multiple subsystems.

III. PWPAT

As mentioned, PWP algorithm approximates each state space segment via a higher order ODE. The choice of segments is carried out in a "training" procedure: from $t = 0$, the original system is reduced at current states point and simulated along the time axis. If the output deviates by a certain distance from the existing trajectory, a new expansion state point is picked up and a set of new reduction parameters are updated. Suppose finally k expansion points $\{x_1, x_2, \cdots, x_k\}$ are chosen from the state space of the original system, each of which has an expression

$$\begin{aligned} E\dot{x} &= f(x_i) + G_{1i}(x - x_i) + G_{2i}(x - x_i) \otimes (x - x_i) \\ &\quad + G_{3i}(x - x_i) \otimes (x - x_i) \otimes (x - x_i) + \cdots + Bu \\ y &= Cx \end{aligned} \tag{8}$$

$$\begin{aligned}\mathscr{A}_2\left(H_2\left(s_1,s_2\right)\right) &= \left(sE-G_1\right)^{-1}\Big(G_2\left(sE\otimes E-G_1\otimes E-E\otimes G_1\right)^{-1}\left(E^{-1}b\right)\otimes\left(E^{-1}b\right)\Big)\\ &= \left\{E,\left[\begin{array}{c|c} G_1 & I_n \\ \hline I_n & 0\end{array}\right]\right\}\cdot\left\{E\otimes E,\left[\begin{array}{c|c} G_1\otimes E+E\otimes G_1 & \left(E^{-1}b\right)\otimes\left(E^{-1}b\right) \\ \hline G_2 & 0\end{array}\right]\right\}\\ &= \left\{\left[\begin{array}{c|c} E & 0 \\ \hline 0 & E\otimes E\end{array}\right],\left[\begin{array}{cc|c} G_1 & G_2 & 0 \\ 0 & G_1\otimes E+E\otimes G_1 & \left(E^{-1}b\right)\otimes\left(E^{-1}b\right) \\ \hline I_n & 0 & 0\end{array}\right]\right\} = \left\{P_1,\left[\begin{array}{c|c} M_1 & F_1 \\ \hline N_1 & 0\end{array}\right]\right\}\end{aligned} \tag{13}$$

where G_{1i}, G_{2i} and $G_{3i}\cdots$ are the first-, second- and higher order derivatives of $f(x)$ at x_i. For ease of illustration, we consider up to the second order. Therefore at each of the expansion point x_i, we have

$$E\dot{x} = f\left(x_i\right)+G_{1i}\left(x-x_i\right)+G_{2i}\left(x-x_i\right)\otimes\left(x-x_i\right)+Bu. \tag{9}$$

By defining $\tilde{x} = x - x_i$, the transfer functions of (9) are the same as (7) except the DC point described by the constant on the right side of the ODE. In order to generate a compact reduced model, associated transform is derived for the special transfer functions form in (7) [11], which is based on the following two theorems:

Theorem 1 *For two square matrices $A_1\in\mathbb{R}^{n_1\times n_1}$ and $A_2\in\mathbb{R}^{n_2\times n_2}$, the associated transform of the Kronecker product of their resolvent matrices in variables s_1 and s_2 is given by*

$$\begin{aligned}&\mathscr{A}_2\left(\left(s_1E_1-A_1\right)^{-1}\otimes\left(s_2E_2-A_2\right)^{-1}\right)\\ &= \left(s(E_1\otimes E_2)-A_1\otimes E_2-E_1\otimes A_2\right)^{-1}.\end{aligned} \tag{10}$$

Theorem 2 *The two-variable association of the univariate transfer function $(s_1E-A)^{-1}b$ is simply $E^{-1}b$, or*

$$\mathscr{A}_2\left(\left(s_1E-A\right)^{-1}b\right) = E^{-1}b. \tag{11}$$

Applying the above two theorems, associated form of transfer functions (7b) can be obtained.

$$\begin{aligned}&\mathscr{A}_2\Big(\left[(s_1+s_2)E-G_1\right]^{-1}G_2\left[H_1(s_1)\otimes H_1(s_2)\right.\\ &\qquad\left.+H_1(s_2)\otimes H_1(s_1)\right]/2)\\ &= \left(sE-G_1\right)^{-1}G_2\left(sE\otimes E-G_1\otimes E-E\otimes G_1\right)^{-1}\\ &\quad\left[\left(E^{-1}b\right)\otimes\left(E^{-1}b\right)\right].\end{aligned} \tag{12}$$

Subsequently, using the often used transfer function notation $\left\{E,\left[\begin{array}{c|c} A & B \\ \hline C & D\end{array}\right]\right\} = C\left(sE-A\right)^{-1}B+D$ to combine (10) and (11), we get (13) on the top of this page. In (13), obviously $\mathscr{A}_2(H_2)$ is recast into a higher order (n^2+n) linear state space. Using similar mechanism, $\mathscr{A}_3(H_3)$ can be carefully derived to be

$$\mathscr{A}_3(H_3) = (sE-G_1)^{-1}G_2\tilde{H}_3(s), \tag{14}$$

where

$$\begin{aligned}\tilde{H}_3(s) &= \left(I_n\otimes N_1\right)\left(sE\otimes P_1-G_1\otimes M_1-M_1\otimes G_1\right)^{-1}\left[\left(E^{-1}b\right)\otimes F_1\right]\\ &\quad+\left(N_1\otimes I_n\right)\left(sP_1\otimes E-M_1\otimes G_1-G_1\otimes M_1\right)^{-1}\left[F_1\otimes\left(E^{-1}b\right)\right],\end{aligned}$$

which can again be put into a linear state space as in (13). The resulting dimension of $H_3(s)$ is $\left(2n^3+2n^2+n\right)$.

Accordingly, the quadratic ODE of (9) can be converted into multiple separated linear ODEs via associated transform. To reduce (9), Arnoldi process is employed on the Krylov subspaces of these linear ODEs to generate several projection bases $V_1\in R^{n\times(k_1+1)}$, $V_2\in R^{n\times(k_2+1)}$ and $V_3\in R^{n\times(k_3+1)}$, where k_1, k_2 and k_3 are the moments matching order numbers of each Krylov subspace.

Algorithm 1 PWPAT algorithm for nonlinear macromodeling.

1: Transient simulation of original system $E\dot{x} = f\left(x\left(t\right)\right)+Bu\left(t\right)$ for $x_1, x_2\cdots x_{end\_training}$.
2: Initialize x_0, $i=1$, $k=0$. A_0 and W_0 are the Jacobian and Hessian of $f(x)$ at $x=x_0$, $K_0=f(x_0)$.
3: Perform NMOR via associated transform on $E_0\dot{x} = A_0x+W_0x\otimes x+K_0+B_0\left(u\right)$ for V_0.
4: Generate initial training model $\hat{E}_0\dot{z} = \hat{A}_0z+\hat{W}_0z\otimes z+\hat{K}_0+\hat{B}_0\left(u\right)$.
5: **while** $i < end\_training$ **do**
6: Transient simulation of training model in step (4) for z_i.
7: **if** $\frac{\|V_{i-1}z_i-x_i\|}{x_i} > \delta$ **then**
8: $k = k+1$.
9: Choose x_i as a new expansion point. Update $x_k = x_i$, E_k, A_k, W_k, B_k and $K_k = f(x_k)$.
10: Perform nonlinear MOR via associated transform on $E_k\dot{x} = A_kx+W_kx\otimes x+K_k+B_k\left(u\right)$ for V_k.
11: Generate training model $\hat{E}_k\dot{z} = \hat{A}_kz+\hat{W}_kz\otimes z+\hat{K}_k+\hat{B}_k\left(u\right)$.
12: Store z_k, $\hat{E}_k$, $\hat{A}_k$, $\hat{W}_k$, $\hat{K}_k$ and $\hat{B}_k$.
13: **end if**
14: **end while**
15: $V = svd\left(\left[V_0V_1\cdots\right]\right)$.
16: Construct the reduced model of the system

$$\hat{E}\dot{z} = \sum_{i=1}^{k}\left(\omega_i\left(z\right)\right)\left(\hat{A}_i(z-z_i)+\hat{W}_i(z-z_i)\otimes(z-z_i)+\hat{K}_i+\hat{B}\left(u\right)\right)$$

$$y = C\left[\sum_{i=1}^{k}\left(\omega_i\left(z\right)\right)\left(x_i+V(z-z_i)\right)\right]$$

in which $w_i\left(z\right) = \frac{\exp\left(\frac{-\beta\|z-z_i\|}{m}\right)}{\sum_{i=1}^{k}\exp\left(\frac{-\beta\|z-z_i\|}{m}\right)}$ where β is some constant (typically we use 25), and $m = \min_i\|z-z_i\|$.

Then, by aggregating the projection bases $[V_1\ V_2\ V_3]$, an orthonormal project basis $V_i \in R^{n\times q}$ $(q \ll n)$ can be formulated. The reduced order model (ROM) generated by associated transform is usually more compact than the ROM generated by conventional weakly NMOR algorithms such as [6, 9, 10]. By singular value decomposition (SVD) on all the segment bases V_i, a uniform projection matrix for the whole system V is generated. Finally, the ROM is obtained by a weighted combination of all these segments such that

$$\hat{E}\dot{z} = \sum_{i=1}^{k} (\omega_i(z)) (\hat{f}(x_i) + \hat{G}_{1i}(z - z_i) + \hat{G}_{2i}(z - z_i) \otimes (z - z_i) + \hat{B}u)$$
$$y = C\left[\sum_{i=1}^{k} (\omega_i(z)) (x_i + V(z - z_i))\right] \quad (15)$$

where $\hat{f}(x_i) = V^T f(x_i)$, $\hat{G}_{1i} = V^T G_{1i} V$, $\hat{G}_{2i} = V^T G_{2i}(V \otimes V)$, $\hat{B} = V^T B$ and $z_i = V^T x_i$.

Algorithm 1 in the last page summarizes the completed PWPAT algorithm.

IV. Numerical Experiments

A. Nonlinear transmission line

We first illustrate with a practical nonlinear transmission line circuit. The original circuit has 100 stages. All resistors and capacitors are set to 1 and the I-V characteristic of the diodes is $i_D = e^{40v_D} - 1$. Using modified nodal analysis (MNA), the circuit can be characterized by 100 differential equations with exponential relationships. The generated models can attain a 15X and 33X speedups for PWPAT and TPWL, respectively, in time-domain simulation. From Fig. 3(b) and Fig. 3(d), although TPWL model shows a faster simulation speed, its accuracy with small signal input is not satisfactory. On the other hand, PWPAT provides much better accuracies for both large and small signal inputs.

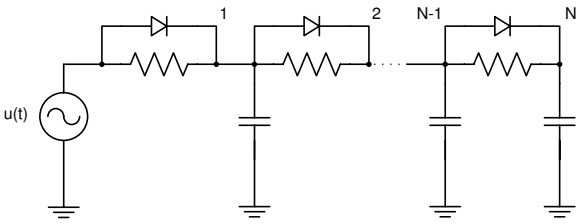

Fig. 2. Example of a nonlinear transmission line.

Local accuracy is important when performing simulations which reflects higher order characteristics, such as 2nd-order and 3rd-order intermodulation products and 1dB compression point. Fig. 4 sweeps both the fundamental and 2nd-order intermodulation products under different input magnitudes. The result verifies that PWPAT model is necessary in performing circuit linearity simulations.

As a comparison, another PWP method via NORM algo-

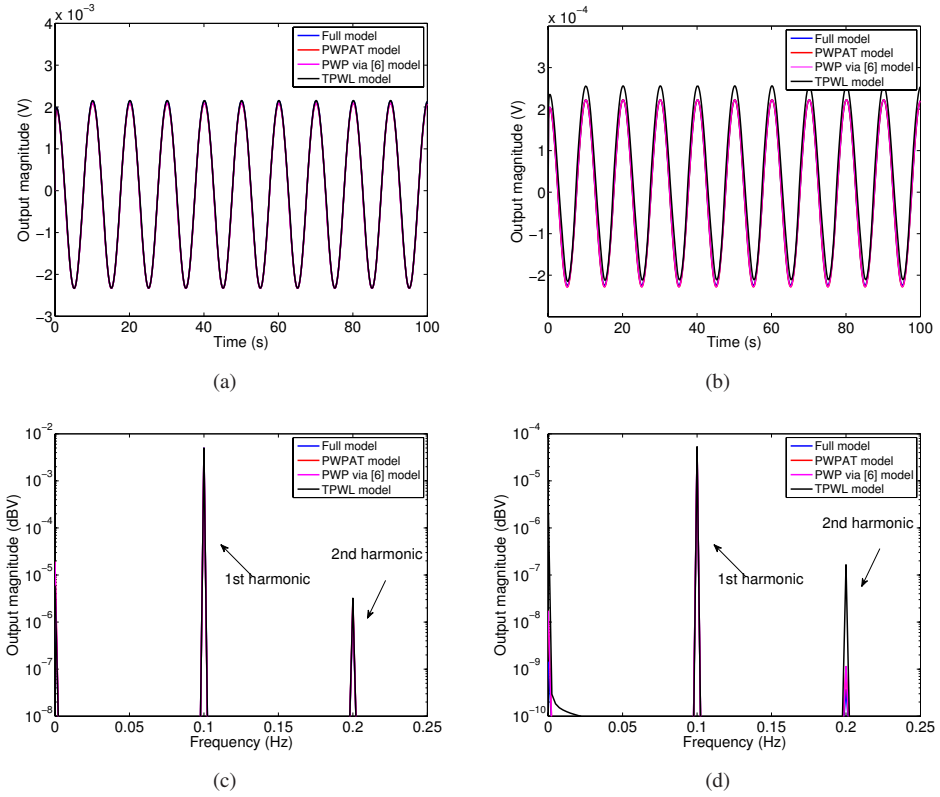

Fig. 3. Comparison between original and reduced models. (a) Large input in time domain. (b) Small input in time domain. (c) Large input in frequency domain. (d) Small input in frequency domain.

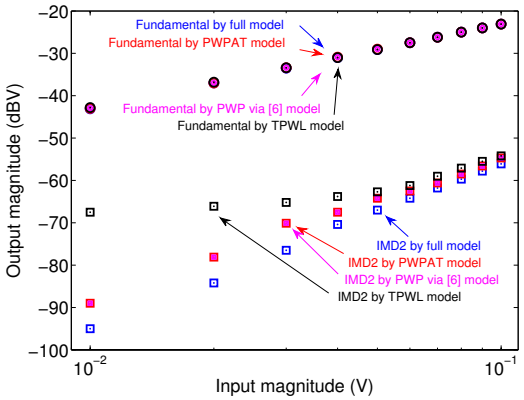

Fig. 4. Fundamental and IMD2 products by original and reduced models.

TABLE I
RESULTS SUMMARY BETWEEN PWPAT, PWP VIA [6] AND TPWL

Large input	Original	PWPAT	PWP via [6]	TPWL
Size	100	15x2	22x2	16x3
Time (Solving ODE)	315.57s	20.54s	25.29s	9.42s
Error $\frac{\|Vz-x\|}{\|x\|}$	—	0.0168	0.0175	0.0125
1st order harmonic	-23.0dBV	-23.1dBV	-23.1dBV	-23.0dBV
2nd order harmonic	-57.0dBV	-55.4dBV	-55.3dBV	-54.9dBV
Small input	**Original**	**PWPAT**	**PWP via [6]**	**TPWL**
Size	100	15x2	22x2	16x3
Time (Solving ODE)	327.39s	20.79s	24.62s	9.57s
Error $\frac{\|Vz-x\|}{\|x\|}$	—	0.0128	0.0145	0.2197
1st order harmonic	-43.0dBV	-43.0dBV	-43.0dBV	-42.8dBV
2nd order harmonic	-94.4dBV	-89.5dBV	-89.3dBV	-67.8dBV

rithms in [6] has also been exercised, with same matching orders k_1, k_2 and k_3. As shown in Table I, the ROMs generated by PWPAT and PWP via [6] demonstrate a similar accuracy, but the dimension of the ROM generated by PWPAT is smaller than the other one. Subsequently, macromodeling by PWPAT not only provides higher order accuracy, but also results in the most compact ROM.

B. Analog buffer

In this example, a CMOS analog buffer circuit is simulated by the proposed algorithm. The small-signal circuit schematic

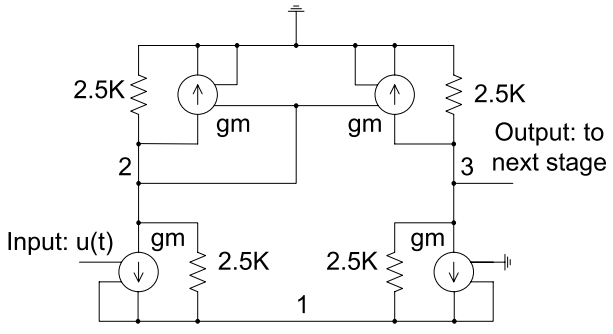

Fig. 5. Example of analog buffer.

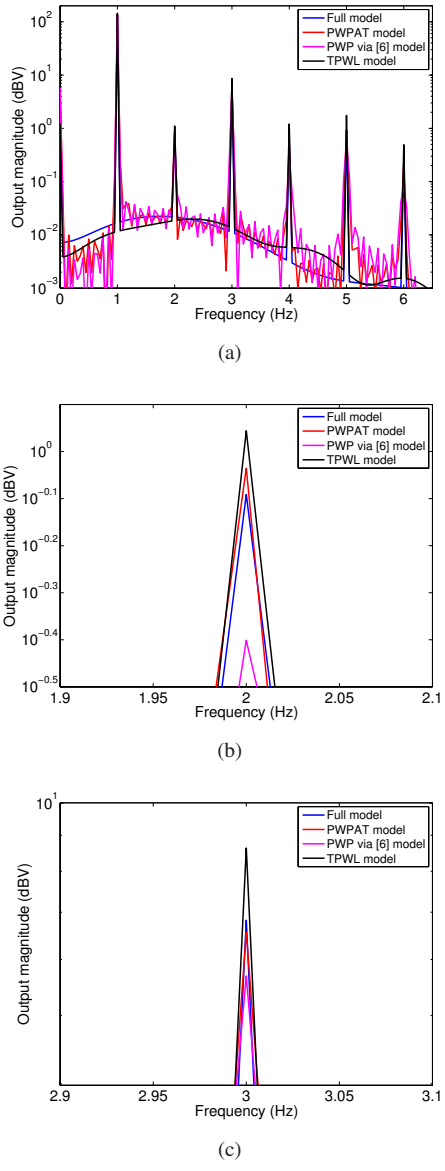

Fig. 6. Simulation of the analog buffer by original and reduced models. (a) Spectrum of the output. (b) 2nd-harmonic. (c) 3rd-harmonic.

is shown in Fig. 5 and it has totally 61 nodes. The transconductance of NMOS and PMOS, g_m, is nonlinear with a polynomial expression

$$i_{ds} = g_{m1}v_{gs} + g_{m2}v_{gs}^2 + g_{m3}v_{gs}^3 + \cdots . \qquad (16)$$

The circuit is reduced by PWPAT, PWP via [6] and TPWL modeling methods into ROM dimensions of 30, 60 and 33, respectively, and placed in the testbench for top-level simulations. Fig. 6(a) plots the spectrum of the final output node. From the zoomed 2nd- and 3rd-harmonic plots in Fig. 6(b) and Fig. 6(c), under similar ROM dimensions, the accuracy superiority of the PWPAT method over TPWL is obvious.

V. CONCLUSION

A novel trajectory piecewise based strongly nonlinear model order reduction algorithm, called PWPAT, has been proposed.

This algorithm combines the benefits of TPWL's global accuracy and local higher order approximations to perform macromodeling of nonlinear circuits. The generated macromodels are crucial when doing simulations calling for higher order characteristics.

Acknowledgments

This work is supported in part by the Hong Kong Research Grant Council under GRF Project 718711E, and in part by the University Research Committee of The University of Hong Kong.

References

[1] L. Pillage and R. Rohrer, "Asymptotic waveform evaluation for timing analysis," *IEEE Trans. on Computer-Aided Design of Integrated Circuits And Systems*, vol. 9, pp. 352–366, Apr. 1990.

[2] P. Feldmann and R. W. Freund, "Efficient linear circuit analysis by Pade approximation via the Lanczos process," *IEEE Trans. on Computer-Aided Design of Integrated Circuits And Systems*, vol. 14, no. 5, pp. 639–649, May 1995.

[3] A. Odabasioglu, M. Celik, and L. T. Pileggi, "PRIMA: Passive reduced-order interconnect macromodeling algorithm," *IEEE Trans. on Computer-Aided Design of Integrated Circuits And Systems*, vol. 17, no. 8, pp. 645–654, Aug. 1998.

[4] J. R. Phillips, "Projection-based approaches for model reduction of weakly nonlinear, time-varying systems," *IEEE Trans. on Computer-Aided Design of Integrated Circuits And Systems*, vol. 22, no. 2, pp. 171–187, Feb. 2003.

[5] C. Gu, "QLMOR: a projection-based nonlinear model order reduction approach using quadratic-linear representation of nonlinear systems," *IEEE Trans. on Computer-Aided Design of Integrated Circuits And Systems*, vol. 30, no. 9, pp. 1307–1320, Sep. 2011.

[6] P. Li and L. Pileggi, "Compact reduced-order modeling of weakly nonlinear analog and RF circuits," *IEEE Trans. on Computer-Aided Design of Integrated Circuits And Systems*, vol. 23, no. 2, pp. 184–203, Feb. 2005.

[7] M. Rewienski and J. White, "A trajectory piecewise-linear approach to model order reduction and fast simulation of nonlinear circuits and micromachined devices," *IEEE Trans. on Computer-Aided Design of Integrated Circuits And Systems*, vol. 22, no. 2, pp. 155–170, Feb. 2003.

[8] N. Dong and J. Roychowdhury, "General-purpose nonlinear model-order reduction using piecewise-polynomial representations," *IEEE Trans. on Computer-Aided Design of Integrated Circuits And Systems*, vol. 27, no. 2, pp. 249–264, Feb. 2008.

[9] J. Roychowdhury, "Reduced-order modelling of linear time-varying systems," in *Intl. Conf. Computer Aided Design*, Nov. 1998, pp. 92–95.

[10] J. Phillips, "Automated extraction of nonlinear circuit macromodels," in *Custom Integrated Circuits Conference*, May 2000, pp. 451–454.

[11] Y. Zhang, H. Liu, Q. Wang, N. H. W. Fong, and N. Wong, "Fast nonlinear model order reduction via associated transforms of high-order volterra transfer functions," in *Design Automation Conference*, Jun. 2012.

[12] C. Gu and J. Roychowdhury, "Model reduction via projection onto nonlinear manifolds, with applications to analog circuits and biochemical systems," in *Intl. Conf. Computer Aided Design*, Nov. 2008, pp. 85–92.

[13] Y. Jiang and H. Chen, "Application of general orthogonal polynomials to fast simulation of nonlinear descriptor systems through piecewise-linear approximation," *IEEE Trans. on Computer-Aided Design of Integrated Circuits And Systems*, vol. 31, no. 5, pp. 804–808, May 2012.

[14] J. K. Lubbock and V. S. Bansal, "Multidimensional Laplace transforms for solution of nonlinear equations," *Proc. IEE*, vol. 116, no. 12, pp. 2075–2082, Dec. 1969.